

Effect of titanium and nitrogen inoculation on the microstructure, mechanical properties and abrasive wear resistance of Hadfield Steels

<http://dx.doi.org/10.1590/0370-44672019730023>

Pablo Enrique Guzman Fernandes^{1,2}

<https://orcid.org/0000-0002-1129-2147>

Leandro Arruda Santos^{1,3}

<https://orcid.org/0000-0001-9172-6429>

¹Universidade Federal de Minas Gerais - UFMG,
Escola de Engenharia, Departamento de Engenharia
Metalúrgica e Materiais,
Belo Horizonte - Minas Gerais - Brasil.

E-mail.: ²pablo.eg.fernandes@gmail.com,

³leandro.arruda@demet.ufmg.br

Abstract

The effect of titanium and nitrogen addition on Hadfield steels was investigated. In order to do this, two grades of steels were produced in terms of titanium and nitrogen addition. The final samples had their microstructure characterized and their mechanical properties were evaluated by uniaxial tensile and Charpy impact tests. Furthermore, the wear resistance was measured by dry sand rubber wheel abrasive tests. Microscopy analyses demonstrated that the precipitation of titanium carbonitrides resulted in a coarse microstructure, with large columnar grains coexisting with equiaxed ones. Consequently, these samples presented lower mechanical properties in comparison with the samples without titanium and nitrogen, which showed a finer microstructure. On the other hand, the presence of hard Ti(C, N) precipitates in the microstructure improved the abrasive wear performance of the steel during the abrasive tests.

Keywords: Hadfield steel, mechanical properties, abrasive wear, titanium and nitrogen inoculation

1. Introduction

It is estimated that the mining industry represents 6.2% of the global energy consumption in the world, being 40% of this consumed energy used to overcome friction. With the development of technologies to promote friction reduction and wear protection, losses regarding this subject can be dramatically reduced. Additionally, the equivalent of 20% of the energy consumed in the mining industry is used to remanufacture and replace worn out parts and equipment due to wear failures (Holmberg *et al.*, 2017).

Hadfield Steels are used as a protection against wear in crushing equipment, due to their combination of high impact resistance and elevated strain hardening capacity. Typically, Hadfield steels have a chemical composition of 1.2%C and 12%Mn, with a Charpy V-notch impact resistance around 140J/cm². In ideal working conditions, the strain hardening

leads to an increase of hardness of the material surface, and consequently, the development of its known wear resistance (Subramanyam *et al.*, 1990).

Despite the consolidated literature regarding the production (Subramanyam *et al.*, 1990; Kuyucak, 2004; Kuyucak *et al.*, 2004) and studying of the deformation mechanisms (Adler *et al.*, 1986; Canadinc *et al.*, 2008; Chen *et al.*, 2017; Dastur; Leslie, 1981; Efstathiou; Sehitoglu, 2010; Karaman *et al.*, 2000) present in Hadfield steels, the relationship between microstructural aspects, such as grain refinement and precipitates, as well as wear resistance are not yet well established. Some authors suggest that the addition of titanium results in grain refinement for Hadfield steels and the increase of wear resistance as a result of a finer microstructure (Limooei; Hosseini, 2012; Magdaluyo *et al.*, 2016; Najafabadi *et al.*, 2014). The precipitation

of Ti(C, N) could contribute to the increase of nucleation sites, and consequently, finer microstructure (Kucharczyk *et al.*, 2003). However, the grain refinement theory of cast metals using inoculation indicates that the lattice mismatch between precipitates and matrix should also be considered (Liu *et al.*, 2017). A low lattice mismatch between matrix and particle can indeed increase the nucleation rate. On the other hand, Siafakas *et al.* (2017) observed that the relationship between γ -iron and Ti(C, N) tends to be incoherent. It could result in fewer nucleation sites and coarser grains when compared with materials presenting coherency between matrix and precipitates.

Thus, the aim of this study was to verify the influence of the addition of titanium and nitrogen on the microstructure, mechanical properties, and abrasive wear resistance of Hadfield steels.

2. Materials and methods

Two grades of Hadfield steels were produced using an open induction melting furnace with 2,000 kg of capacity with the metal being poured using a ladle with a capacity of 300kg. One heat was produced for each grade, and the treatment of inoculating titanium and nitrogen was performed in the ladle. The samples without the addition of Ti and N were deoxidized in the induction furnace with 0.1% (wt.%) of calcium silicon and 0.03% (wt.%) of aluminum. On the other hand, the samples containing

titanium and nitrogen were deoxidized using the same procedure, and ferrotitanium, nitrogen-rich ferromanganese and aluminum were added to the ladle during the metal transfer from the furnace, with the objective to add 0.1% of Ti (wt.%), 0.03% of N (wt.%) and 0.04% of Al (wt.%). Aluminum was added with the objective to induce the precipitation of titanium carbonitrides. Three Y-blocks (approximately 10kg) for each composition were cast using a pouring temperature of 1480 °C, and the excess

metal was returned to the furnace. The chemical composition was determined by optical emission spectroscopy using a SPECTROMAXx spectrometer. Samples for chemical composition analysis were cut from one of the cast Y-blocks for each produced grade. Table 1 indicates the chemical composition of the produced samples. Samples 12Mn and 12MnTi are in accordance with grade A of ASTM A128 standard and samples 12MnCr and 12MnCrTi with grade C of the same standard.

Table 1 – Chemical composition of the test samples (wt.%).

Sample ID	C	Mn	Cr	Ti	N	Al	P
12Mn	1.26	12.68	0.58	0.01	0.0113	0.03	0.053
12MnTi	1.26	12.99	0.58	0.10	0.0116	0.06	0.053
12MnCr	1.31	12.67	1.60	0.01	0.0138	0.02	0.060
12MnCrTi	1.31	13.10	1.61	0.11	0.0151	0.06	0.064

Samples were then solution heat treated at 1090 °C for 3 hours of soaking time followed by water quenching. After the standard metallographic procedure of grinding and polishing, some samples were selected and etched using a 2:2:1 (H₂O, HCl, H₂O₂) solution for macrographic investigation, whereas another group of samples was etched using a 4% Nital solution (Kuyucak, 2004) in order to characterize their microstructure.

The specimens for tensile tests, V-notched Charpy impact testing and dry sand rubber wheel abrasion tests were cut and prepared by electrical discharge machining (EDM), with geometry and dimensions given by ASTM-E8M, ASTM-E23 and ASTM-G65 standards, respectively. Tensile tests were performed at room temperature on an INSTRON 5583 device, using a strain rate of 5x10⁻⁴ s⁻¹ until rupture. Charpy V-notch impact

test were performed also at room temperature on a Wolpert PW30/15 equipment using a load of 300J. And finally, abrasion tests were performed according to procedure A of the standard ASTM-G65: 130 N load 6000 revolutions, using sand with an AFS fineness number between 40 and 50.

The microstructure and wear surfaces were analyzed using a FEI Inspect S50 scanning electron microscope equipped with an EDAX EDS System.

3. Results and discussion

3.1 Macrostructural and microstructural characterization

Figure 1 shows the macrographs of the produced samples, which depicts details of the effect of titanium and nitrogen addition on the material's morphology. The samples with the addition of Ti and N presented a significant increase in the columnar solidification zone and equiaxed grain size. The co-

lumnar morphology observed in the samples containing Ti and N additions is related to the presence of incoherent precipitates, which is in accordance with the findings published by Sifakas *et al.* (2017). Essentially, these precipitates are titanium carbonitrides, $Ti(C, N)$, which were detected by SEM/EDS (see Figure

2). Furthermore, the same SEM/EDS analysis also indicated that part of these titanium carbonitrides precipitated with the help of aluminum oxide inclusions as seen in Figure 2. Previous studies demonstrate that these precipitates are formed before the solidification of the matrix (Sifakas *et al.*, 2016, 2017).

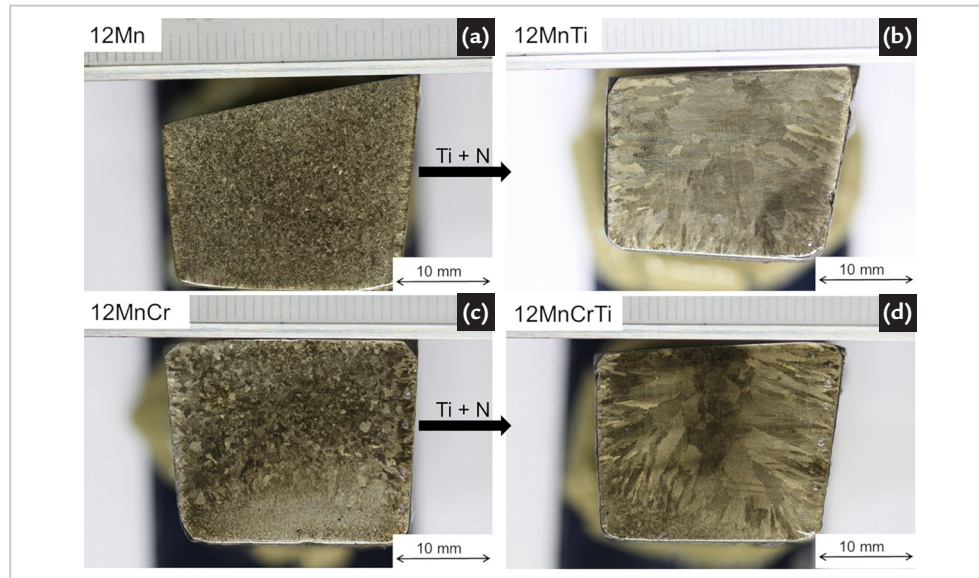


Figure 1 – Macrographs of the test samples. (a) sample 12Mn; (b) sample 12MnTi; (c) sample 12MnCr; (d) sample 12MnCrTi.

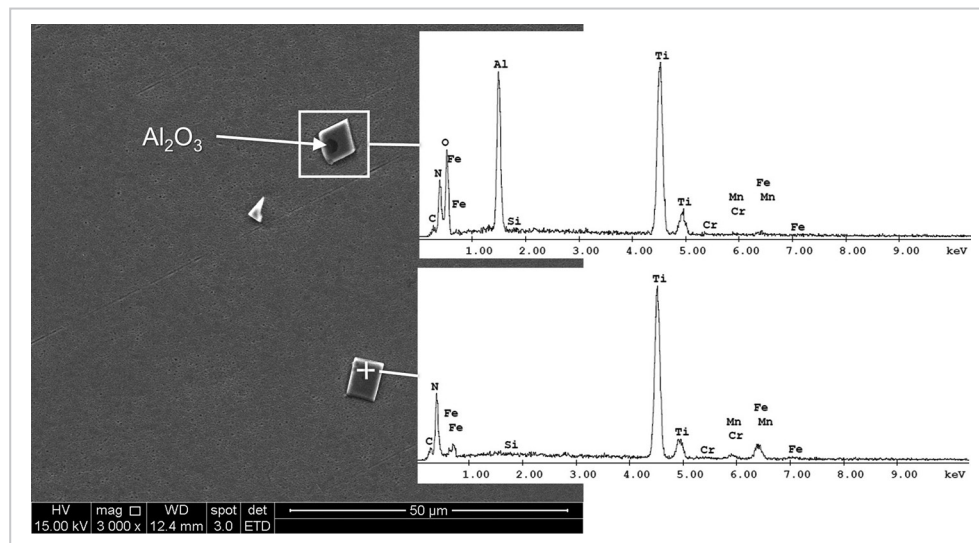


Figure 2 – SEM images and EDS analysis of titanium carbonitrides on sample 12MnCrTi.

Figure 3 shows the presence of titanium carbonitrides inside an interdendritic carbide and at grain boundaries. The formation of $Ti(C, N)$ from an aluminum oxide inclusion can also be observed, as previously discussed. This morphology suggests that $Ti(C, N)$ precipitates preferentially remained in the liquid phase and are entrapped by dendritic arms or neighboring

grains during the solidification process. Furthermore, Sifakas *et al.* (2017) demonstrated that spinel ($MnAl_2O_4$ - $MgAl_2O_4$) had a lower lattice mismatch with γ -iron and could be a more effective grain refiner. It may explain the morphology of the samples 12Mn and 12MnCr (without the addition of titanium and nitrogen), whose presence of spinel inclusions from the furnace

lining material could have led to the observed grain refinement effect. On the other hand, the formation of complex titanium carbonitrides from the aluminum oxide precipitates increases the mismatch between precipitates and the matrix, resulting in fewer nucleation sites and coarser grains. However, further investigation is necessary to evaluate this hypothesis.

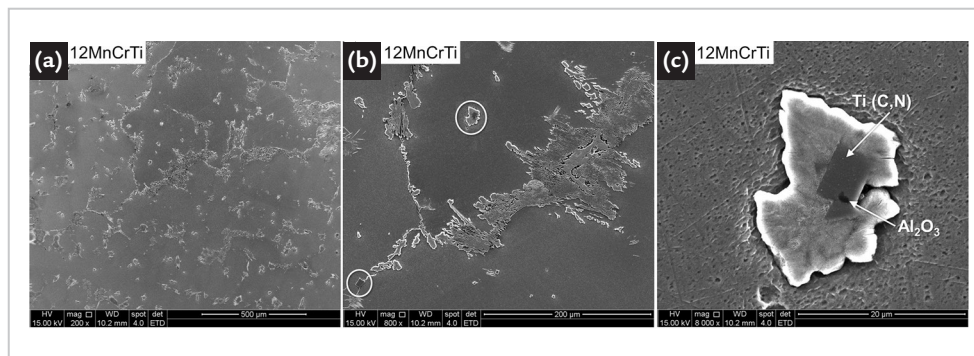


Figure 3 – SEM images from sample 12MnCrTi without heat treatment. Titanium precipitates are observed inside interdendritic carbides and on grain boundaries.

3.2 Mechanical test results

Figure 4 shows the tensile test curves obtained for each of the studied alloys, while Table 2 presents a summary of the mechanical property values as well as the Charpy impact results. The two factors that most affected tensile tests results were chemical

composition and grain size. The addition of chromium increased yield strength of both 12MnCr and 12MnCrTi materials, which is consistent with classical literature (Subramanyan *et al.*, 1990). Grain size negatively affected both yield strength and strain

hardening capacity. Coarsened grains as a consequence of the addition of titanium and nitrogen reduced the yield strength of both 12MnTi and 12MnCrTi samples. The effect of grain size on yield strength is expected according to the Hall-Petch law.

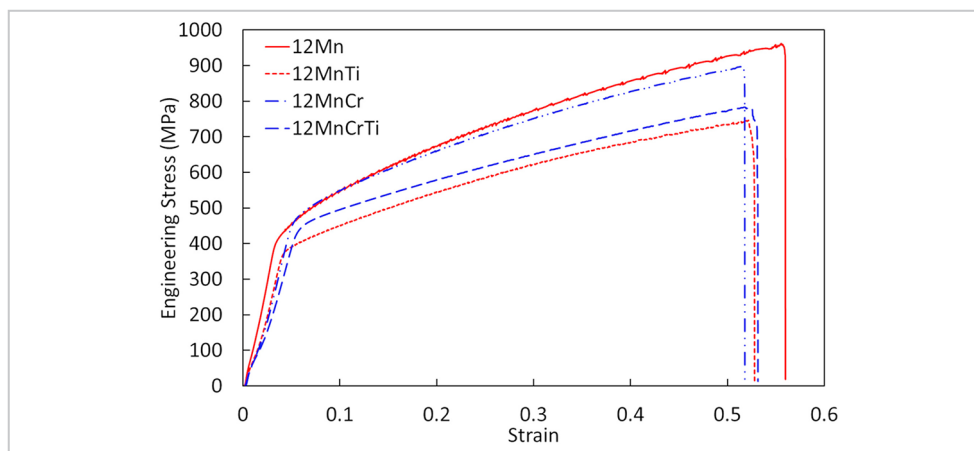


Figure 4 – Engineering stress-strain curves of the test samples.

Table 2 – Mechanical and wear test results of the test samples, as well as mean value and standard deviation of 3 samples.

Sample ID	Yield Strength (MPa)	Tensile Strength (Mpa)	Elongation (%)	Impact toughness (J/cm ²)
12Mn	415 ± 2	955 ± 19	46 ± 1	171±1
12MnTi	378 ± 7	728 ± 84	44 ± 5	179 ± 26
12MnCr	471 ± 2	903 ± 10	42 ± 3	165 ± 4
12MnCrTi	444 ± 5	795 ± 34	42 ± 1	148 ± 11

The strain hardening capacity was negatively affected by the increase in grain size, which is in agreement with the results observed by Karaman *et al.* (2000) and Venturelli *et al.* (2018). Nevertheless, these authors diverge on their conclusion about the mechanism that leads to this difference in strain hardening capacity. Venturelli *et al.* (2018) attributed the increase in the strain hardening coefficient in fine mi-

crostructures to an increase in the twin density. On the other hand, Karaman *et al.*(2000) suggested that the increase in the strain hardening coefficient in a fine grain microstructure is related to a stronger slip activity. Figure 5 compares the differences between the microstructures of samples 12MnCr and 12MnCrTi after the tensile tests. Mechanical twins can be observed in the samples, and due to the deep etching

applied to the samples, the presence of deformations bands can also be observed (Qian *et al.*, 2011). The different patterns of deformation can be attributed to the difference in the degree of deformation in different grains or different regions of the same grain. Even in the same grain, different patterns may also be generated because of different local constraints resulting from the grain boundaries and the surrounding grains.

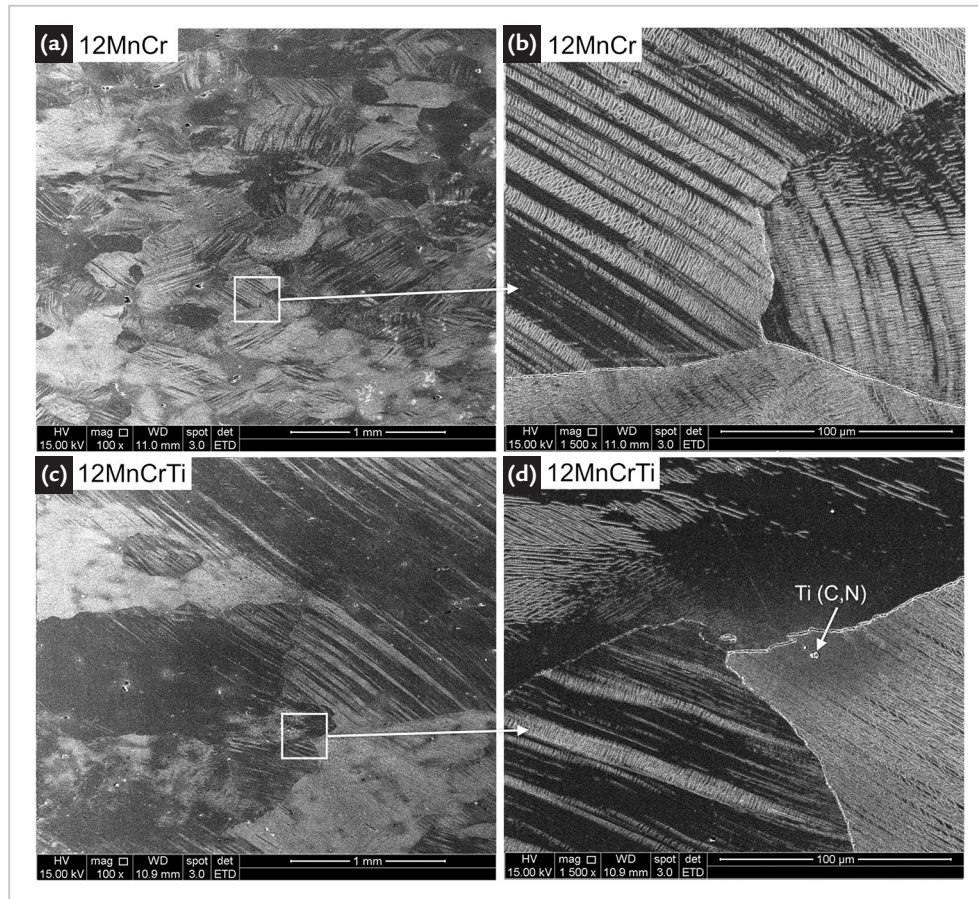


Figure 5 – SEM images of the samples after tensile tests. (a) and (b) sample 12MnCr; (c) and (d) samples 12MnCrTi.

The effect of titanium and nitrogen addition on the impact resistance led to contradictory observations. The 12Mn sample depicted a small increase in im-

compact resistance, whereas sample 12MnCr presented a slight decrease in the same property. Despite this decrease observed in the 12MnCrTi case, the obtained results

are consistent with the expected values for Hadfield steels (Subramanyan et al., 1990; Kuyucak, 2004; Venturelli *et al.*, 2018).

3.3 Wear characterization

Table 3 and Figure 6 show the results of dry sand rubber wheel abrasion tests. For both of the studied

steels, it is suggested that the addition of titanium and nitrogen significantly increased the wear resistance. Samples

12Mn and 12MnCr had a volume loss of 22% and 14% greater than those with Ti and N, respectively.

Table 3 – Volume loss during abrasion tests (mm³). Mean value and standard deviation of 4 samples.

Sample ID	0 - 10 min	10 - 20 min.	20- 30 min.	Total Volume Loss
12Mn	26.70 ± 1.43	24.86 ± 0.95	24.79 ± 0.87	76.36 ± 2.39
12MnTi	21.94 ± 2.25	21.18 ± 1.52	19.29 ± 3.50	62.41 ± 5.90
12MnCr	25.24 ± 1.86	24.02 ± 0.60	23.96 ± 0.67	73.22 ± 2.43
12MnCrTi	21.78 ± 1.68	22.08 ± 1.20	20.34 ± 1.94	64.21 ± 4.04

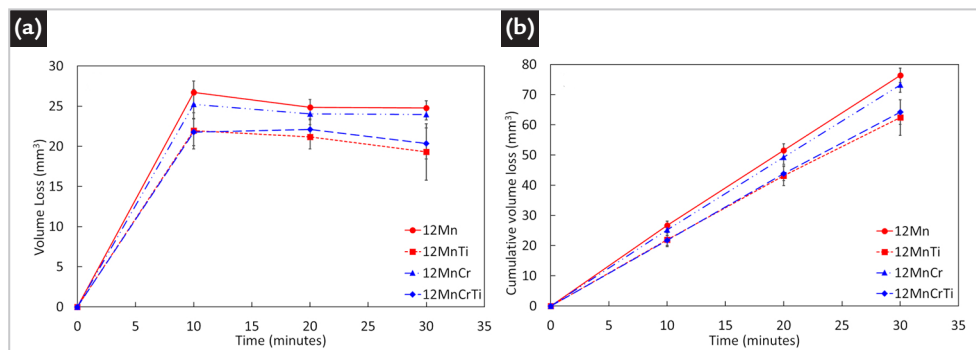


Figure 6 – Dry sand abrasion test results. (a) volume loss during tests; (b) cumulative volume loss during tests.

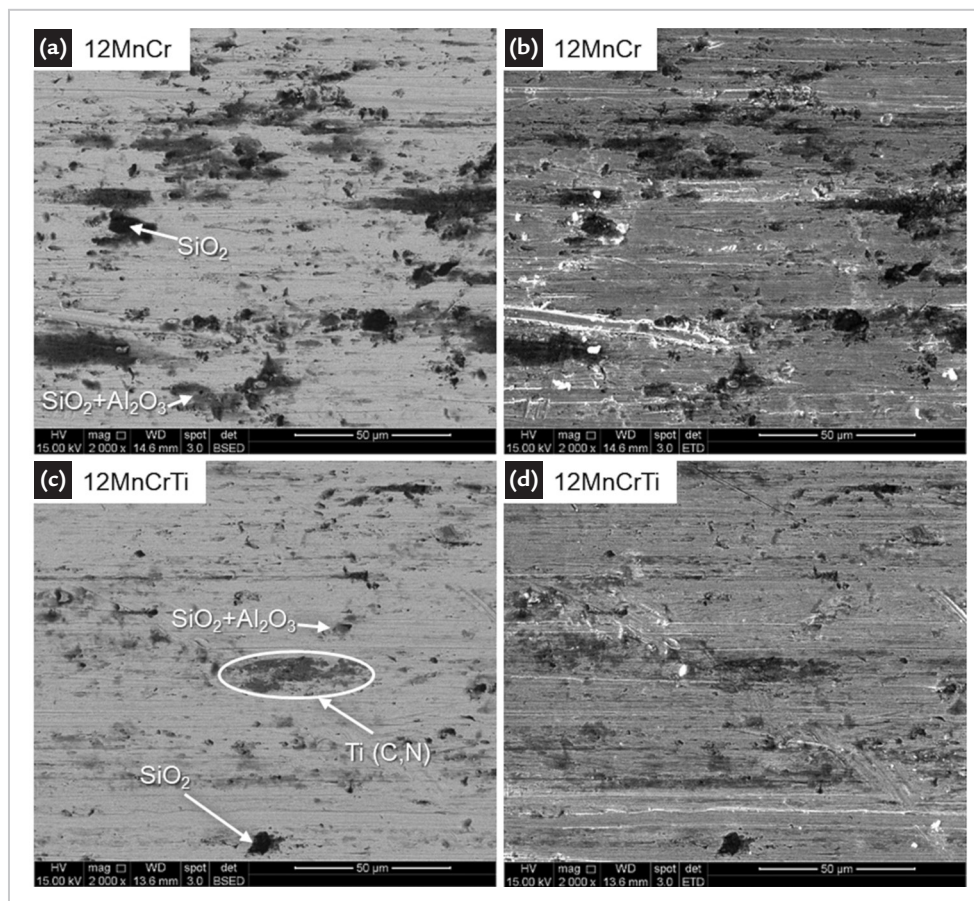


Figure 7 – SEM images and EDS analysis of worn surface of the tested samples.

(a) BSE image of sample 12MnCr; (b) SE image of sample 12MnCr; (c) BSE image of sample 12MnCrTi; (d) SE image of sample 12MnCrTi.

SEM analysis from the worn surfaces of samples 12MnCr and 12MnCrTi (Figures 7) indicates the wear mechanisms of microploughing and microcutting, which are related to the presence of grooves with and without build-up materials on their edges (Tressia et al., 2017). The worn surface of sample 12MnCr exhibits the presence of embedded abrasive particles in the matrix at different stages of aggregation, indicated by the secondary electron images showing particles at different depths.

In sample 12MnCrTi, it was possible to observe the presence of Ti(C, N) precipitates on the worn surfaces. The precipitates were fractured by the abrasive particles, but the fractured

particles remained at the sample matrix. Thus, it is reasonable to assume that the presence of hard Ti(C, N) precipitates distributed in matrix contributed to the increase in the wear resistance. Those precipitates protected the surface against the action of the abrasive particles, reducing the volume loss during the wear tests. It could be estimated that the precipitates represent a 0.2% volume fraction in the matrix (Zhang, 1993). These strongly embedded precipitates may absorb a part of the external load and reduce the sliding action of abrasive particles, acting as a barrier. Carbides or hard precipitates embedded in a soft matrix can substantially reduce the abrasive wear loss (Zum Gahr, 1987).

Further investigation is needed to evaluate the mechanical behavior of Hadfield steels under gouging or impact abrasion conditions. It is expected that a higher strain hardening capacity may provide a harder work surface and, consequently, a material with more resistance against wear. This was not observed in the wear results obtained in this study, suggesting that the observed precipitates in the samples with Ti and N additions play an important role in the wear mechanisms of these materials. The competition between a superior strain hardening capacity and the abrasive wear resistance provided by Ti(C, N) precipitates should be evaluated in future studies.

4. Conclusions

1 – Microstructural characterization revealed that the addition of titanium and nitrogen on two grades of Hadfield steel resulted in a microstructure with coarser columnar and equiaxed grains.

2 – The presence of Ti(C, N) pre-

cipitates inside the interdendritic carbides suggests that Ti(C, N) precipitates are entrapped by dendritic arms or neighboring grains during the solidification process.

3 – Tensile properties were negatively affected, with a significant loss on both

yield and tensile strength. Elongation and impact resistance were not significantly affected.

4 – The presence of hard Ti(C, N) precipitates increased the wear resistance in dry sand rubber wheel abrasion tests.

Acknowledgements

This work was supported by Conselho de Nível Superior - Brasil (CAPES) - Finance Code 001.

References

- ADLER, P. H.; OLSON, G. B.; OWEN, W. S. Strain hardening of Hadfield manganese steel. *Metallurgical and Materials Transactions A*, v. 17, n. 10, p. 1725-1737, 1986.
- ASTM INTERNATIONAL. *ASTM A128 / A128M-93(2012)*: standard specification for steel castings, austenitic manganese. West Conshohocken: ASTM International, 2012.
- CANADINC, D.; EFSTATHIOU, C.; SEHITOGLU, H. On the negative strain rate sensitivity of Hadfield steel. *Scripta Materialia*, v. 59, n. 10, p. 1103-1106, 2008.
- CHEN, C. et al. Effect of N+Cr alloying on the microstructures and tensile properties of Hadfield steel. *Materials Science and Engineering A*, v. 679, n. June 2016, p. 95-103, 2017.
- DASTUR, Y. N.; LESLIE, W. C. Mechanism of work hardening in Hadfield manganese steel. *Metallurgical transactions. A, Physical metallurgy and materials science*, v. 12 A, n. 5, p. 749-759, 1981.
- EFSTATHIOU, C.; SEHITOGLU, H. Strain hardening and heterogeneous deformation during twinning in Hadfield steel. *Acta Materialia*, v. 58, n. 5, p. 1479-1488, 2010.
- HOLMBERG, K. et al. Global energy consumption due to friction and wear in the mining industry. *Tribology International*, v. 115, p. 116-139, 2017.
- KARAMAN, I. et al. Deformation of single crystal hadfield steel by twinning and slip. *Acta Materialia*, v. 48, n. 6, p. 1345-1359, 2000.
- KARAMAN, I. et al. Modeling the deformation behavior of hadfield steel single and polycrystals due to twinning and slip. *Acta Materialia*, v. 48, p. 2031-2047, 2000.
- KUCHARCZYK, J. W.; FUNK, K. R.; KOS, B. *Grain-refined austenitic manganese steel casting having microadditions of vanadium and titanium and a method of manufacturing*. US Patent 6572713. 2003.
- KUYUCAK, S. Austenitic manganese steel castings. In: ASM INTERNATIONAL. *ASM Handbook Volume 9: metallography and microstructures*. ASM International, 2004. p. 701-708.
- KUYUCAK, S.; ZAVADIL, R.; GERTSMAN, V. Heat-treatment processing of austenitic manganese steels. In: WORLD FOUNDRY CONGRESS, 66., 2004, Istanbul. *Proceedings[...]*. Istanbul, Turkey: Turkish Foundrymen's Assn, 2004.
- LIMOUEI, M. B.; HOSSEINI, S. *Optimization of properties and structure with addition of titanium in Hadfield steels*. In: INTERNATIONAL CONFERENCE ON METALLURGY AND MATERIALS, 21., 2012, Brno, Czech Republic. *Proceedings[...]*. Brno, Czech Republic: 2012.
- LIU, S. et al. Simultaneously increasing both strength and ductility of Fe-Mn-C twinning-induced plasticity steel via Cr/Mo alloying. *Scripta Materialia*, v. 127, p. 10-14, 2017.
- MAGDALUYO JR, E. R.; AUSA, M. S.; TINIO, R.J. Effect of titanium on gouging abrasion behavior and hardness of austenitic manganese steel. In: AO, S. I.; YANG, G. C.; GELMAN, L.(ed.) *Transactions on Engineering Technologies*. Singapore: Springer, 2016. cap.1, p. 73-81.
- NAJAFABADI, V. N.; AMINI, K.; ALAMDARLO, M. B. Investigating the effect of titanium addition on the wear resistance of Hadfield steel. *Metallurgical Research & Technology*, v. 111, n. 6, p. 375-382, 2014.
- QIAN, L.; FENG, X.; ZHANG, F. Deformed microstructure and hardness of Hadfield high manganese steel. *Materials Transactions*, v. 52, n. 8, p. 1623-1628, 2011.
- SIAFAKAS, D. et al. Particles precipitation in Ti- and Al-Deoxidized Hadfield steels. *Steel Research International*, v. 87, n. 10, p. 1344-1355, 2016.
- SIAFAKAS, D. et al. The Influence of deoxidation practice on the As-Cast grain size of austenitic manganese steels. *Metals*, v. 7, n. 186, p. 1-10, 2017.
- SUBRAMANYAM, D. K.; SWANSIGER, A. E.; AVERY, H.S. Austenitic Manganese Steels. In: ASM INTERNATIONAL. *ASM Handbook Volume 1, Properties and Selection: irons, steels, and high-performance alloys*. ASM International, 1990. p. 822-840.
- TRESSIA, G.; PENAGOS, J. J.; SINATORA, A. Effect of abrasive particle size on slurry abrasion resistance of austenitic and martensitic steels. *Wear*, v. 376-377, p. 63-69, 2017.
- VENTURELLI, B. N.; ALBERTIN, E.; AZEVEDO, C. R. F. The effect of the austenite grain refinement on the tensile and impact properties of cast Hadfield steel. *Materials Research*, v. 21, n. 5, p. 1-8, 2018.
- ZHANG, S. Titanium carbonitride-based cermets: processes and properties. *Materials Science and Engineering A*. v. 163, n.1, p. 141-148, 1993.
- ZUM GAHR, K. H. *Microstructure and wear of materials*. Amsterdam: Elsevier, 1987. 560 p. (Tribology Series, 10)

Received: 4 March 2019 - Accepted: 2 September 2019.



All content of the journal, except where identified, is licensed under a Creative Commons attribution-type BY.